

Supplement of Atmos. Chem. Phys., 20, 12515–12525, 2020
<https://doi.org/10.5194/acp-20-12515-2020-supplement>
© Author(s) 2020. This work is distributed under
the Creative Commons Attribution 4.0 License.



Supplement of

Large contribution of organics to condensational growth and formation of cloud condensation nuclei (CCN) in the remote marine boundary layer

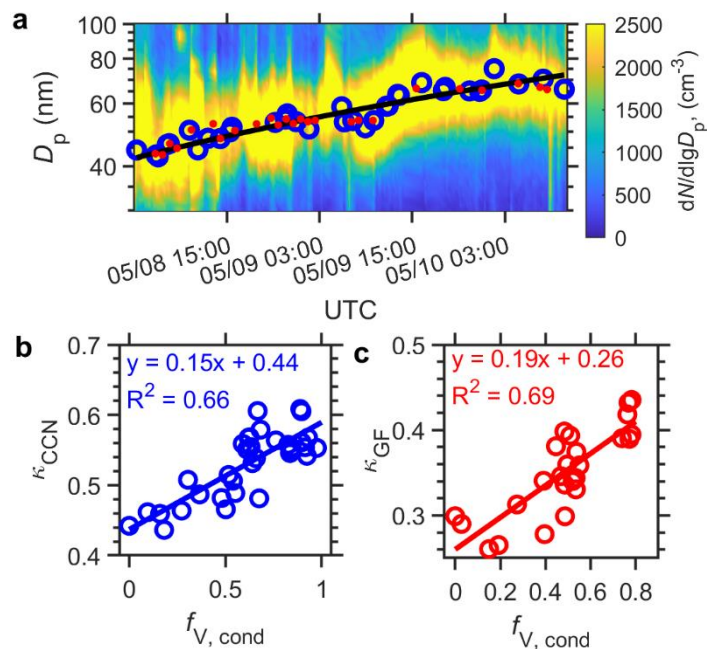
Guangjie Zheng et al.

Correspondence to: Jian Wang (jian@wustl.edu)

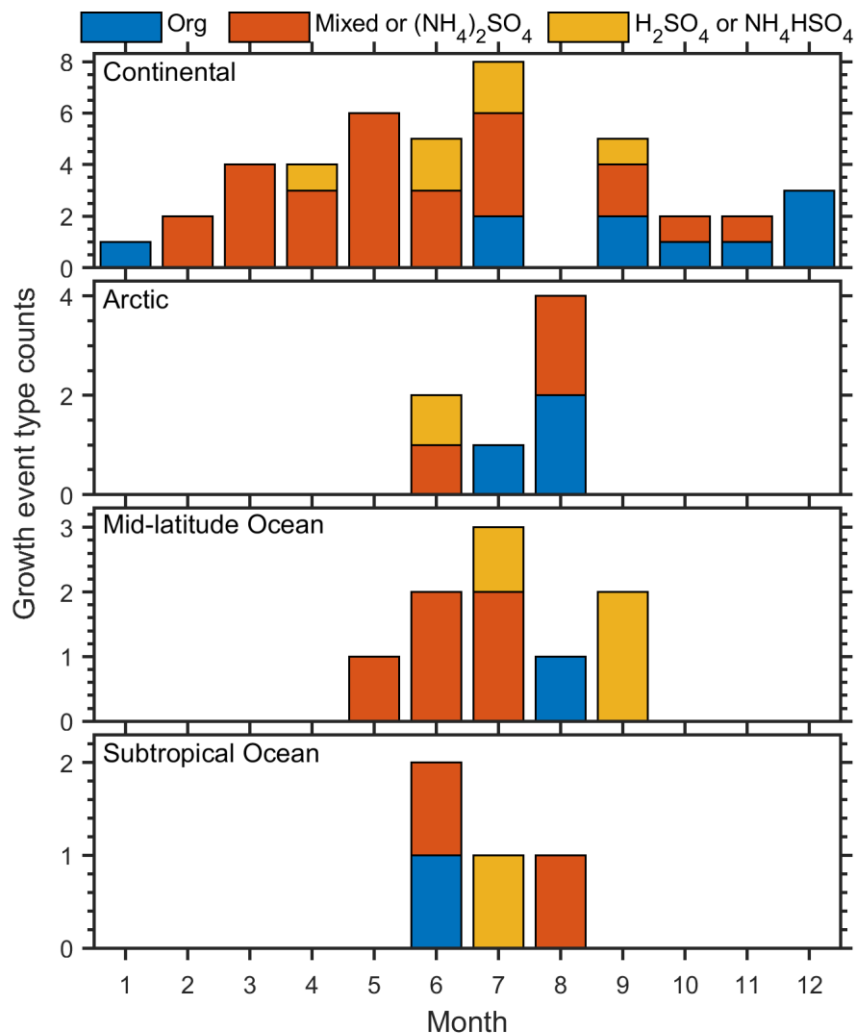
The copyright of individual parts of the supplement might differ from the CC BY 4.0 License.

S1. Classification of air mass origins

The origins of the air masses arriving at the ENA site are classified based on the air mass back-trajectories. Here 10-day
15 back-trajectories are simulated using the HYSPLIT 4 model (Stein et al., 2015) every hour starting from 500 m above the
ground level, with the input of NCEP Global Data Assimilation System (GDAS) meteorological data. The back-trajectories
are then classified into four categories using the following approach. First, all air masses that had passed over the North
America ($130^{\circ} \sim 60^{\circ} \text{ W}$, $35^{\circ} \sim 62^{\circ} \text{ N}$) or northern Europe ($-10^{\circ} \text{ W} \sim 30^{\circ} \text{ E}$, $35^{\circ} \sim 62^{\circ} \text{ N}$) are classified as “Continental
origins”. Second, air masses that passed over the Arctic regions (latitude higher than 62° N) are then denoted as “the Arctic”.
20 Third, among the remaining air masses, those passed over subtropical oceans (latitude lower than 35° N) at times 6 - 150 h
prior are classified as “Subtropical origins”. Last, all other air masses are considered as “mid-latitude Atlantic”. The
dominant air mass origin during a given growth event is designated as the air mass category of that event.



30 **Figure S1. An example case of deriving $\kappa_{c,CCN}$ and $\kappa_{c,GF}$ for the same growth event.** (a) Aerosol size distribution during the growth event. The blue circles and red dots represent lognormal-fitted Aitken mode diameters at the times of the SCCN and HTDMA measurements, respectively. The black line shows the growth of the Aitken mode diameter during the event. (b) A $\kappa_{c,CCN}$ value of 0.59 (i.e., the sum of slope and intercept) is derived from the linear fitting of κ_{CCN} vs. $f_{V,cond}$. This value falls in the intermediate- $\kappa_{c,CCN}$ category. (c) A $\kappa_{c,GF}$ value of 0.45 is derived from the variation of κ_{GF} following the same approach. Major condensing species of this case is determined to be $(\text{NH}_4)_2\text{SO}_4$ (see detailed discussions in section 5 of the main text).



35 Figure S2. Monthly distribution of condensational growth event and the dominant condensing species for each type of air mass origins.

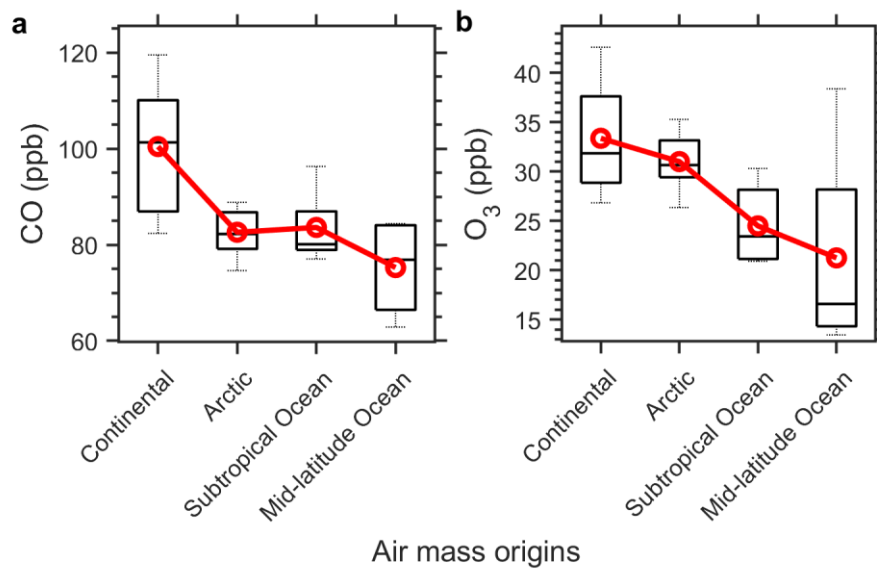


Figure S3. Trace gas mixing ratios in air masses of different origins. (a) CO and (b) O₃.

40

45

References

- Chang, R. Y. W., Slowik, J. G., Shantz, N. C., Vlasenko, A., Liggio, J., Sjostedt, S. J., Leaitch, W. R., and Abbatt, J. P. D.: The hygroscopicity parameter (κ) of ambient organic aerosol at a field site subject to biogenic and anthropogenic influences: relationship to degree of aerosol oxidation, *Atmos. Chem. Phys.*, 10, 5047-5064, 10.5194/acp-10-5047-2010, 2010.
- 50 Johnson, G. R., Ristovski, Z., and Morawska, L.: Method for measuring the hygroscopic behaviour of lower volatility fractions in an internally mixed aerosol, *Journal of Aerosol Science*, 35, 443-455, <https://doi.org/10.1016/j.jaerosci.2003.10.008>, 2004.
- Massoli, P., Lambe, A. T., Ahern, A. T., Williams, L. R., Ehn, M., Mikkilä, J., Canagaratna, M. R., Brune, W. H., Onasch, T. B., Jayne, J. T., Petäjä, T., Kulmala, M., Laaksonen, A., Kolb, C. E., Davidovits, P., and Worsnop, D. R.: Relationship between aerosol oxidation level and hygroscopic properties of laboratory generated secondary organic aerosol (SOA) particles, *Geophysical Research Letters*, 37, 10.1029/2010gl045258, 2010.
- 55 Petters, M. D., and Kreidenweis, S. M.: A single parameter representation of hygroscopic growth and cloud condensation nucleus activity, *Atmos. Chem. Phys.*, 7, 1961-1971, 10.5194/acp-7-1961-2007, 2007.
- Schmale, J., Henning, S., Decesari, S., Henzing, B., Keskinen, H., Sellegri, K., Ovadnevaite, J., Pöhlker, M. L., Brito, J., Bougiatioti, A., Kristensson, A., Kalivitis, N., Stavroulas, I., Carbone, S., Jefferson, A., Park, M., Schlag, P., Iwamoto, Y., Aalto, P., Äijälä, M., Bukowiecki, N., Ehn, M., Frank, G., Fröhlich, R., Frumau, A., Herrmann, E., Herrmann, H., Holzinger, R., Kos, G., Kulmala, M., Mihalopoulos, N., Nenes, A., O'Dowd, C., Petäjä, T., Picard, D., Pöhlker, C., Pöschl, U., Poulain, L., Prévôt, A. S. H., Swietlicki, E., Andreae, M. O., Artaxo, P., Wiedensohler, A., Ogren, J., Matsuki, A., Yum, S. S.,
- 60 Stratmann, F., Baltensperger, U., and Gysel, M.: Long-term cloud condensation nuclei number concentration, particle number size distribution and chemical composition measurements at regionally representative observatories, *Atmos. Chem. Phys.*, 18, 2853-2881, 10.5194/acp-18-2853-2018, 2018.
- Stein, A. F., Draxler, R. R., Rolph, G. D., Stunder, B. J. B., Cohen, M. D., and Ngan, F.: NOAA's HYSPLIT Atmospheric Transport and Dispersion Modeling System, *Bulletin of the American Meteorological Society*, 96, 2059-2077, 10.1175/bams-d-14-00110.1, 2015.
- 70 Tang, M., Guo, L., Bai, Y., Huang, R.-J., Wu, Z., Wang, Z., Zhang, G., Ding, X., Hu, M., and Wang, X.: Impacts of methanesulfonate on the cloud condensation nucleation activity of sea salt aerosol, *Atmospheric Environment*, 201, 13-17, <https://doi.org/10.1016/j.atmosenv.2018.12.034>, 2019.